# Accepted Manuscript

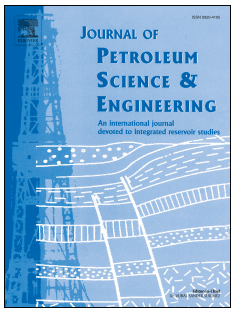


The influence of magnetic fields on calcium carbonate scale formation within ethylene glycol solutions at regeneration conditions

Ammar Al Helal, Adam Soames, Stefan Iglauer, Rolf Gubner, Ahmed Barifcani

PII: S0920-4105(18)30850-7

DOI: 10.1016/j.petrol.2018.09.100

Reference: PETROL 5364

To appear in: *Journal of Petroleum Science and Engineering*

Received Date: 30 July 2018

Revised Date: 28 September 2018

Accepted Date: 29 September 2018

Please cite this article as: Al Helal, A., Soames, A., Iglauer, S., Gubner, R., Barifcani, A., The influence of magnetic fields on calcium carbonate scale formation within ethylene glycol solutions at regeneration conditions, *Journal of Petroleum Science and Engineering* (2018), doi: https://doi.org/10.1016/j.petrol.2018.09.100.

# The Influence of Magnetic Fields on Calcium Carbonate Scale Formation within Ethylene Glycol Solutions at Regeneration Conditions

*Ammar Al Helal*[*†], *Adam Soames*[*], *Stefan Iglauer*[**], *Rolf Gubner*[*], *Ahmed Barifcani*[*]

*WA School of Mines: Minerals, Energy and Chemical Engineering, Curtin University, Perth W.A., Australia
**School of Engineering, Edith Cowan University, Joondalup W.A., Australia
† Corresponding Author

**Abstract**

One of the most discussed topics related to the effects of external magnetic fields (MF) on aqueous solutions is the influence on the scale formation of calcium carbonate ($CaCO_3$). However, the extent of the effect of these forces on the scale formation in the non-aqueous solutions has not been investigated so far. So MFs will be applied to non-aqueous mixtures to find out the behavior of scale formation. This study presents the results of inorganic scale formation within MEG solutions containing $Ca^{2+}$ and $HCO_3^-$ ions, which has been investigated using both static and dynamic scale loop (DSL) evaluation techniques. Furthermore, the influence of MFs on scale formation using the dynamic technique has also been studied. Results were generated using brine/MEG solutions exposed to an external MF produced by a 0.65 Tesla Neodymium magnet for 2.5 seconds. The degree of scale formation was examined by measuring the pressure build-up across a capillary coil as scale was developed. Moreover, differences in $CaCO_3$ morphologies were evaluated for the exposed and blank trials via the DSL technique and compared with the results obtained from the static scale evaluation method.

The results of this research have demonstrated that the short exposure (2.5 seconds) to a powerful MF can significantly reduce scale-formation in the rich MEG solutions within the capillary coil. This is due to the alteration of the proton spin inversion in the field of diamagnetic salts. Furthermore, a significant difference in $CaCO_3$ morphology was observed for the scale formed during dynamic and static conditions. The generating results help to reduce the use of chemical scale inhibitors with MEG solution during the gas hydrate treatments, especially when the concentration of MEG in formation water is low and scale formation is more likely to occur.

Keywords: Magnetic fields, MEG, Calcium carbonate, Morphology, Scale formation, Dynamic scale loop.

## 1.0 Introduction

Calcium carbonate is a common mineral scale experienced in a wide range of industries including water treatment[1-2], paper mill industries[3], cooling water systems[4], natural gas transportation pipelines and MEG regeneration systems following the breakthrough of formation water[5-6]. The formation of $CaCO_3$ occurs upon the surface of heat transfer equipment operating at high temperatures, such as heat exchangers and reboilers, leading to reduced heat transfer efficiency[7] and potential blockages or restrictions of flow along the inner surfaces of pipelines and tubing[2, 8]. Several studies have been conducted to investigate the scale formation behavior of $CaCO_3$ by examining various characteristics including crystalline phase, size distribution, and morphology[9-11]. The saturation index (SI) of calcium and carbonate ions have been the subject of extensive prior studies and represent a key factor in determining the tendency of $CaCO_3$ to form[1, 12].

Muryanto, et al. [9] reported that $CaCO_3$ crystals are formed in three anhydrous polymorphs: calcite, aragonite, and vaterite. Calcite is known as the most stable form of $CaCO_3$ crystal while aragonite and vaterite exhibit poor

thermodynamic stability with the potential to convert to calcite after readjustment of certain conditions including fluid pH, temperature, supersaturation, and the presence of additives[9, 13]. For instance, Hu, et al. [13] reported that at pH 9.0, the anhydrous polymorph (vaterite) is more likely to form compared to the hydrated polymorphs of $CaCO_3$ such as monohydrate and hexahydrate (ikaite), which forms at high pH conditions of approximately 13.4 and greater within low temperature[13]. However, in the presence of phosphate additives, the ikaite polymorph is more likely to precipitate at pH 9[13].

In the last decade, the morphology of $CaCO_3$ has been extensively investigated following the application of MFs [14-16]. Silva, et al. [16] for instance, summarized the most significant results including the possibility of obtaining a morphology that has a lower tendency to attach to the walls of water-conveying pipes or the promotion of homogeneous precipitation of $CaCO_3$. However, most of these studies have focused on aqueous solutions as part of attempts to modify scale formation in water systems. As such, little to no investigation has been conducted on the anti-scalent potential of MFs for use in MEG systems containing mineral ions, an application relevant to the hydrocarbon and natural gas industries.

MEG is used extensively in natural gas transportation pipelines as an inhibitor to prevent the formation of natural gas hydrates[17-18]. The use of MEG as a hydrate inhibitor is seeing increasing usage over other traditional hydrate inhibitors such as methanol due to its ability to be regenerated efficiently and reused reducing operational costs[17, 19]. However, in such applications, several problems may arise following the breakthrough of formation water and subsequent introduction of mineral salts into the regeneration loop[15, 18]. The introduction of divalent cations including calcium, magnesium, and barium, pose a scaling risk within critical systems including subsea pipelines, and MEG injection points[20] as well as within MEG regeneration systems operating at a higher temperature such as reboilers[17, 21]. Scaling within the MEG loop and associated systems can be controlled by careful control of system pH or by injection of suitable scaling inhibitors[21-22].

Flaten, et al. [10] claimed that the presence of MEG alongside water affects the supersaturation ratio due to changes in activity coefficients and the solubility of the dissolved salts. Therefore, the presence of MEG within brine solution may influence the morphology of $CaCO_3$ at the wellhead and within the pipeline under continuous flow conditions[23-24]. There is ample precedent to suggest that an increase in MEG weight fraction can decrease the growth rate of $CaCO_3$ and influence the polymorphism, transformation, and crystal size distribution[25]. Moreover, Flaten, et al. [10] have reported that the morphology of the $CaCO_3$ changed at various MEG concentrations and temperatures from calcite to vaterite. The reason behind this behavior is that the activity-based supersaturation ratio represents the actual driving force of $CaCO_3$ precipitation within MEG solution[26].

In aqueous glycol solutions, Rozhkova, et al. [27] proved that the results of the separation of MEG from the saline solutions by ionic exchange membranes improved significantly when electrolytes were present. They attributed this improvement to the apparent changes in the strength of hydrogen bonds between the OH groups of the MEG and the H groups of the water molecules. To describe this phenomenon more adequately, there is a clear reduction in the energy of hydrogen bonds between water and MEG, causing a rise in the MEG molecules mobile rates during the ionic separation process. Thus, the hydrogen bond between water-MEG has been ruptured by the presence of electrolytes that have created strong bonds with water molecules forming the first hydration shell (refer to Figure 1). These bonds are often stronger than the hydrogen bonds formed between the

water molecules and the OH group of MEG, where the large size of the MEG molecules usually causes hydrogen bonds to weaken and then rupture[27-28]. Therefore, any manipulation or modification of the hydration shell surrounding the electrolytes can distort the hydrogen bonds between both the water and the MEG molecules.

The majority of the published fundamental studies presented a precise description of this shell in aqueous solutions, which they defined as a layer of water molecules arranged around the cations and anions linked to them by ion-dipole forces[29-30]. The thickness of the hydration shell often varies according to the size of the ions and the density of the electronic charge, giving it spatial and dynamic properties in the liquid phase[29]. Several studies have indicated an inverse proportional relationship between the thickness of the hydration shell and the ionic mobility in aqueous solutions and a proportional relationship with the valence[31]. Previous literature has demonstrated the possibility of competition between the molecules of MEG and water molecules to form solvation shell in saline solution[27, 32]. Therefore, the use of external forces such as the MFs may be able to induce some significant changes in the thickness of the hydration shell within the MEG solution.

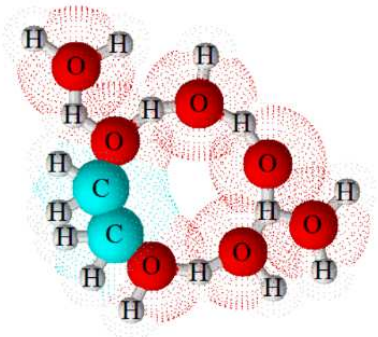

Figure 1 – (A) Hydrogen and covalent bonding of the MEG – water – $Na^+$ ion system as Rozhkova, et al. [27] proposed. Images were generated using ACD/ChemSketch Freeware software [33].

This study evaluates the inhibitory performance of MFs on $CaCO_3$ growth at different MEG concentrations (50 and 80% vol.). Additionally, the EC and pressure variation were monitored and recorded continuously to evaluate the scale formation performance following MF exposure. All trails were conducted with the same initial mineral ions concentration and reboiler skin temperature of approximately 150°C. The experiments were carried out using the DSL system with/without applying an MF source installed after mixing the calcium and bicarbonate ions. Jar tests were also conducted, but without magnetic treatment to provide a reference $CaCO_3$ scale morphology under static conditions.

## 2.0 Experimental Methodology

### 2.1 Experimental Equipment and Chemicals

#### 2.1.1 Brine Solutions

Two MEG solutions as shown in Table 1 were used in this study to evaluate the effects of MF treatment on scale formation at 50 and 80% by volume MEG fractions. Each experiment utilized equal concentrations of $Ca^{2+}$ and $HCO_3^-$ ions (750ppm) with the cationic and anionic species prepared separately within two individual containers to prevent premature reaction. The main reason behind the selection of these volume fractions is the prevalence

of these percentages in MEG regeneration plants. The MEG concentration after induction at the wellhead is often 40 to 60% by volume[34-36], while post-regeneration is often exceeded 80% by volume of MEG[35-36] so that it can be recirculated and re-injected into the wellheads for reuse.

The cationic and anionic charges of all MEG-brine solutions were adjusted by the addition of NaCl as per Table 2. The two MEG volume fractions were utilized to simulate aqueous glycolic solutions at various MEG to water volume fractions at the same ionic strength to assess the effect of MFs treatment on the calcium and bicarb $Ca^{2+}$ and $HCO_3^-$ ions within MEG solution. Jar cell trials were conducted within this study to compare the scale formation morphology of 0, 50 and 80% by volume of MEG solution with DSL technique but at 30 and 150°C. Jar cell trials could not be controlled at 150°C without using autoclave device due to the high evaporation rate, which changed the volume fraction of MEG. The mathematical model described by Al Helal, et al. [37] was used to measure the volume fraction of the glycolic solutions after adding mineral salts to ensure that the initial volume fraction of MEG before each test was correct.

**Table 1 - Experiments for the exposed and blank tests of DSL technique and non-exposed Jar test technique at different conditions**

| Trial No. | Vol. % of MEG | Temperature (°C) | Technique | Magnetic Fields |
|---|---|---|---|---|
| 1 | 50 | 150 | DSL | Yes |
| 2 | 50 | 150 | DSL | No |
| 3 | 80 | 150 | DSL | Yes |
| 4 | 80 | 150 | DSL | No |
| 5 | 0 | 150 | Jar | No |
| 6 | 0 | 30 | Jar | No |
| 7 | 50 | 150 | Jar | No |
| 8 | 50 | 30 | Jar | No |
| 9 | 80 | 150 | Jar | No |
| 10 | 80 | 30 | Jar | No |

### 2.1.2 Chemicals Used

To produce the brine-MEG solutions, ultra-deionized water (18.2MΩ cm) was used for all experiments. The prepared solutions were sparged with $N_2$ gas to avoid contamination by $CO_2$ gas. The brine-MEG solutions consisted of, $MgCl_2.6H_2O$ powder (>99 wt. %), $CaCl_2.2H_2O$ powder (>99 wt. %), $NaHCO_3$ powder (99.7 wt. %), NaCl powder (99.7 wt. %), MEG solution (99.9 wt. %) that provided by Chem-Supply (reagent grade). The pH of injected solutions (i.e. cation and anion solutions) were adjusted by using few drops of 0.1 N of NaOH to maintain the initial pH conditions.

**Table 2 – Brine + MEG + Water concentrations for sets of 50% and 80% by volume of MEG**

| Total Ions | Anion Solution, mg/L | Cation Solution, mg/L | Mixed Solution, mg/L |
|---|---|---|---|
| $Na^+$ | 10600 | 10600 | 10600 |
| $Mg^{2+}$ | 0 | 100 | 50 |
| $Cl^-$ | 15475 | 19293 | 17384 |
| $Ca^{2+}$ | 0 | 1500 | 750 |
| $HCO_3^-$ | 1500 | 0 | 750 |
| pH | 8.2 | 6.34 | |

## 2.2 Magnetic Field Device

An N45SH magnet was used in this study due to its high maximum energy product to affect scale formation operation. The diametrically magnetized orientation was selected due to its flexibility to utilize. Furthermore, it

was placed before the mixing tubing coil before exposing the $Ca^{2+}$ and $HCO_3^-$ solutions to the heating chamber as shown in Figure 2. The cylindrical shape of the magnet orientation incorporates a small hole through the center generating rich MFs. Due to the small gap between the magnetic poles of the cylindrical shape, which reached about 0.1588 cm, the magnetic field strength will reach its maximum strength. This intensive strength will contribute to the modification of some thermodynamic characteristics of the mixture passing through it. The MF intensity of the cylindrical magnet was measured by using a Gauss-meter provided by the Wutronic instrument from Germany. The N45SH magnet specifications and dimensions outlined in Table 3.

**Table 3 - Magnet specifications and dimensions**

| Properties | Specification |
|---|---|
| Dimensions of Magnet | 7.62 cm OD, 0.1588 cm ID, 10.16 cm Thickness |
| Materials and Grade | NdFeB and N45SH |
| Plating/Coating | Ni-Cu-Ni (Nickle) |
| Direction of Magnetization | Diametrically magnetized |
| Maximum operating temperature | 150°C, ±5°C |
| Generated Residual Flux Density Brmax | 13.499 Tesla |
| The Maximum Energy Product BHmax | 44.384 Megagauss Oersted (MGOe) |
| Magnetic susceptibility of water molecules ($\chi$) | $-12.63*10^{-10}$ $m^3/mol$[38] |
| Magnetic strength (H) | $5.27*10^5$ A/m |
| Magnetic flux density (B) | 0.6500 T |

### 2.2.1 Magnetic Fields Validation

Several hypotheses have been proposed to validate the effects of MFs on the thermodynamic properties of hydration shell. For instance, the expression of volumetric density of magnetic energy ($\rho_E$) has been utilized to evaluate the direct potential of external MFs energy to break down the H-bonds of free water molecules[39]. This expression represents the relationship between the magnetic susceptibility of water molecules ($\chi$) and Magnetic strength (H) and Magnetic flux density (B) of the applied magnetic device. The relationship can be expressed as such: -

$$\rho_E = \frac{\delta E_B}{\delta V} = \frac{\chi_{water} * H * B}{2} \quad \ldots 1$$

Where $E_B$ denotes the generated energy from the MFs that applied to the H-Bonds. By using the magnetic specification that is listed in Table 3, the generated energy ($E_B$) from the MFs was estimated at approx $4.33*10^{-6}$ J/mol. The calculated value of $E_B$ was compared with the weakest H-bond energy of free water (5.43 kJ/mol[39]), which is found as such interval:

$$\frac{E_B}{E_{H-bonds}} = 4.43 * 10^{-5}$$

The comparison concluded that the effect of the external MF on the modification of the thickness of the hydration shell is not based on the generated magnetic energy effect. However, Another explanation has been proposed by Madsen [40] which is related to the proton transfer from hydrogen carbonate to water molecules, due to proton spin inversion in the external MF. Moreover, MF effects were also described in terms of changes in the hydration of carbonate ions which might directly alter the polymorph phase equilibrium throughout the precipitation. As a result, the external magnetic field can cause weakening, distorting and alteration in the

number of H-bond that generating between of water molecules and ions. Hence, affecting water molecules structure and its reaction potential with dissolved ions to form hydration shell.

### 2.3 Scanning Electron Microscopy (SEM) analyses

Scanning electron microscope (SEM) analysis was used to identify the morphology of $CaCO_3$ of the exposed and the blank trials samples within different MEG concentration as described in Table 1 and Table 2. The discharge solution of each test was collected and filtered using a 0.22µm syringe filter. The filter papers were subsequently dried to remove any residual fluid. The filter papers were then coated with 5nm platinum to allow analysis by SEM. SEM analysis of the dried samples was then generated using a Zeiss NEON, operating at 10 to 5 kV. Based on the energy dispersive spectroscopy (EDS), the scale formed was identified as polymorphs of $CaCO_3$.

### 2.4 Experimental Setup of DSL Techniques

The trials were performed to investigate the scaling tendency of MEG-Brine solutions containing $HCO_3^-$ and $Ca^{2+}$ ions in the presence of an MF using the dynamic technique, model MinDSL 1725-M from PSL Systemtechnik Germany (refer to Figure 2). The DSL apparatus measures the differential pressure (ΔP) build-up across an inside capillary coil using a pressure detector placed at the inlet and outlet of the capillary coil with an accuracy of ±0.009 bar. An increase in the ΔP across the capillary tube is indicative of the scale formation as the flow of solution is hindered. To investigate the influence of the MF on $CaCO_3$ formation, the ΔP across the capillary coil was monitored and measured until full blockage of the coil occurred as indicated by an increase in the ΔP recorded by the pressure detector. The time recorded for each experiment to attain full blockage of the capillary coil was used to assess the tendency of the MEG-brine solution to form $CaCO_3$.

The dynamic apparatus is illustrated in detail in Figure 2 with specifications outlined in Table 3. The DSL pipelines and instruments were isolated to prevent changes in the operating temperature, brine solutions, and measurements of each trial. The cation and anion solutions were pumped separately into the dynamic apparatus through a Y shaped mixing stream by using two high-pressure pumps at room temperature. The entire flow rate for the cation and anion solutions was set at 300 ml/hr. At room conditions, the scale formation rate should be very slow that it allows the study to evaluate the effects of MF on $CaCO_3$ precipitation by following particle mechanism. The dynamic apparatus contains two individual stainless-steel coils; the first coil used to provide mixing of the MEG-brine solution. Following mixing within the primary coil, the MEG-brine solution is then passed through the center of a cylindrical magnet for a total time of 2.5 seconds with an MF flux density of approximately 0.650 Tesla at the center as shown in Figure 4 and Table 2. The second coil exposed the mixture to a heating room to accelerate the scale formation (refer to Table 3). The experimental conditions like temperature and flow rate were controlled and monitored by using the winDSL software. This study investigated the effects of particle mechanism and Lorentz force in $CaCO_3$ deposit using DSL method.

The temperature of the heating room was set at 150°C (±1°C) during testing using a digital interface controller. A temperature of 150°C was selected to simulate the skin temperature of the MEG regeneration column reboiler unit. A back-pressure regulator valve was placed on the outlet line of the testing capillary coil to set the ΔP across the capillary coil. An EC and pH probes were installed to the discharge tubing line to record the variation in pH and EC measurements after the MF exposure, as per Table 4 and Figure 2.

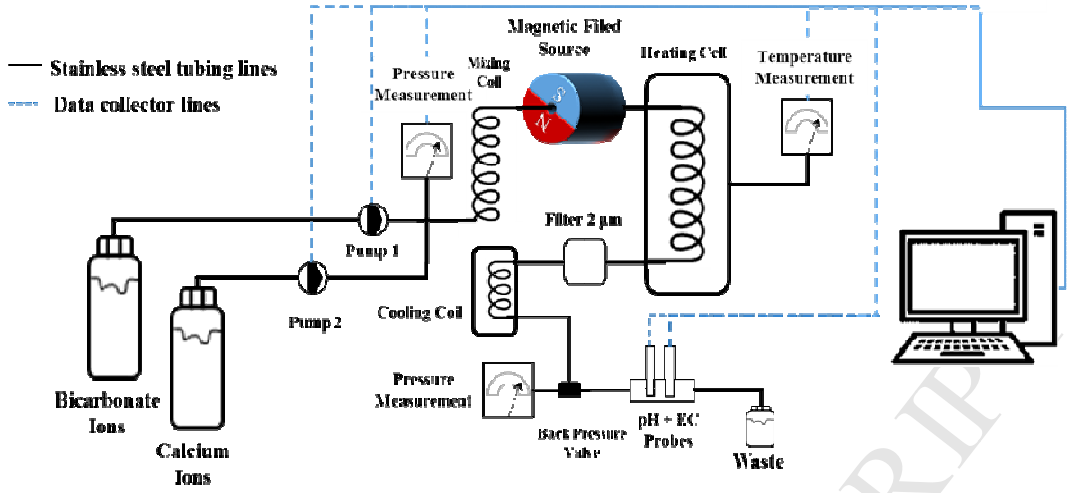


Figure 2 - Schematic of the DSL system

**Table 4 - DSL Specifications**

| Component | Specifications | Notes |
|---|---|---|
| Higher pressure pumps | 0 – 300 ml/hr, ±0.6 ml/hr | Data-logger |
| Mixing Capillary Coil | 10.0 cm Length, 3.171 mm OD and 1.01 mm ID | Stainless steel 316 |
| Test Capillary Coil | 100 cm Length, 1.411 mm OD and 0.76 mm ID | Stainless steel 316 |
| Back Pressure Valve Range | 0 – 172 bar, ±0.01bar | Data-logger |
| Operating Pressure Range | 1 bar to 172 bar | Regulating |
| Operating Heating Chamber | +30 to +250°C, ±0.1°C | Regulating |
| pH-meter | 1-14 | Data-logger |
| Electrical Conductivity meter | 0 – 1000 mS/cm, ±0.1% | Data-logger |
| Micro Filter | 2 Microns | Stainless steel |

### 2.5 Experimental Setup of Jar Cell Techniques

Closed jar testing was conducted to form different crystals of $CaCO_3$ at different MEG concentrations and temperature levels. The jar tests were conducted using the same brine solution compositions used for the DSL trials to evaluate the difference in scale formation morphology compared to that produced using the dynamic process of the DSL system. The experimental temperatures were set at 30°C, and 150°C to form different $CaCO_3$ structures and were exposed to the respective temperature for a period of one hour. The operating temperature was maintained by using an autoclave system having an accuracy of ±2°C, refer to Figure 3. Operation at 150°C was performed under a pressure of 3.0 bar to prevent boiling of the MEG solution. The $CaCO_3$ crystals formed were immediately filtered, dried and subsequently analyzed using SEM to distinguish the difference in the morphologies of the $CaCO_3$.

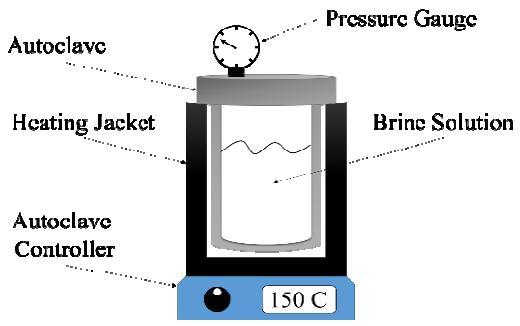


Figure 3 - Schematic Diagram of Jar Cell Techniques (Autoclave)

## 3.0 Results and Discussions

### 3.1 Influence of Magnetic fields on Scale Formation at 80 vol. % MEG Solution

To evaluate the impact of MF exposure on the scale formation tendency of $CaCO_3$ with MEG solution, 80 vol. % MEG solutions containing an equivalent concentration of $Ca^{2+}$ and $HCO_3^-$ ions was exposed to MFs as discussed in Section 2.4. For comparison purposes, blank trials were conducted using the same 80 vol. % MEG solutions with no exposure to the MF. The trails exposed to the MF and corresponding blank tests have been plotted in Figure 4 with respect to the change in ΔP across the capillary coil with time. Overall, 8 trials were performed for both the blank and exposed tests, with the average results plotted, error bars have been included demonstrating one standard deviation of the 8 tests away from the average result.

A consistent sharp rise in ΔP across the capillary coil was observed for trials exposed to the MFs, whilst in comparison, a more gradual rise in ΔP followed by a sharp increase which occurred during blank tests. The sharp increase in ΔP is demonstrative of the capillary coil becoming fully blocked following the formation of scale. The duration time required for the blank tests to experience complete tube blockage was significantly longer than those trials exposed to the MF. As such, it is evident that exposure to the MF has promoted the formation of $CaCO_3$ scale within the 80 vol. % of MEG.

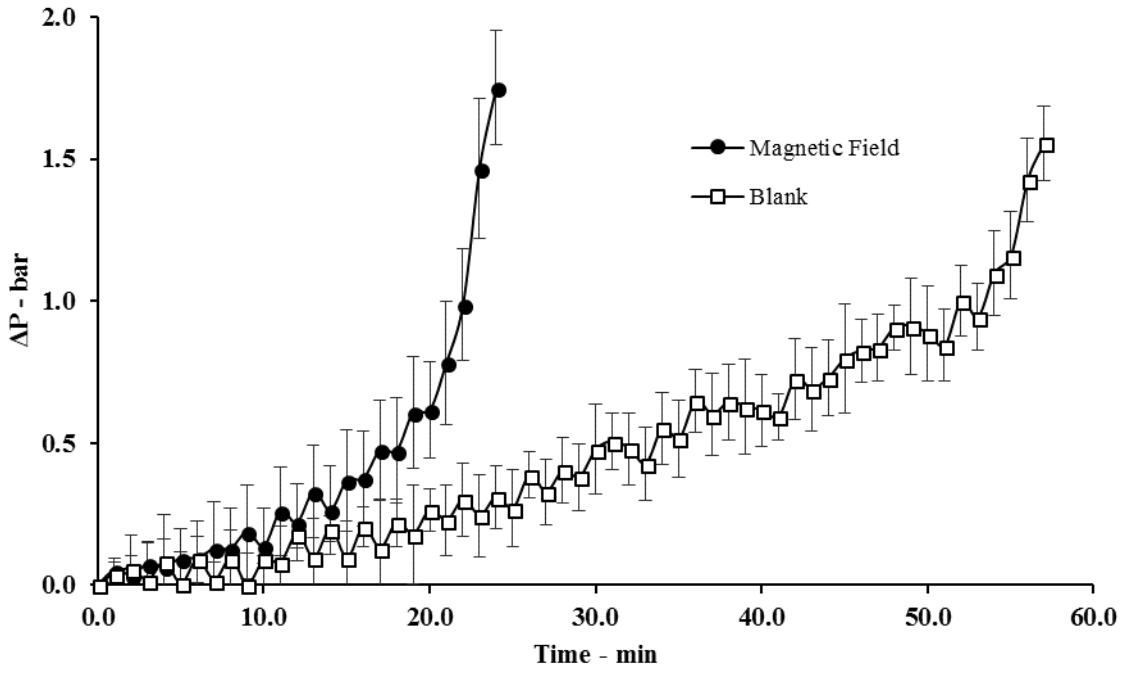


Figure 4 - Effect of MF exposure on the tendency of equal concentration of $Ca^{2+}$ and $HCO_3^-$ solution within 80 vol. % MEG to form scale

Furthermore, the EC of equal concentrations of bicarbonate-calcium solutions established a similar behavior exhibited during the studies by Al Helal, et al. [1] and Szczes, et al. [41] following exposure to an MF. As shown in Figure 5, the application of the MF to equal bicarbonate-calcium concentration 80 vol. % MEG solution has directly decreased the EC readings when compared with the corresponding blank samples results. The results of the magnetically exposed trials are consistent with the conclusions of Hasaani, et al. [42] who reported a similar change in EC of $Ca^{2+}$ - $HCO_3^-$ solution following experience to an MF. These changes were attributed to

thermodynamic changes that altered the thickness of the hydration shell around those ions[16, 43-44]. Therefore, the generated result could suggest that the hydrated layer of the ions was influenced by exposure to the MF, and hence the electrophoretic activity of the electrolytes within 80 vol. % MEG decreased.

Such a decrease in EC may occur due to the bonding of MEG molecules with aqueous solution leading to weakening the H-bonds of water-water molecules[27] (refer to Figure 6). As a result, the weakening of hydrogen bonds tends to impact the hydration shell thickness around dissolved ions[45-46]. Meanwhile, a number of publications stated that the MF effect led to an increase in EC of the aqueous solutions[1, 41, 47]. Furthermore, Silva, et al. [16] reported that less hydrated cations adhere more strongly to anions and vice versa after exposure to MFs within the aqueous solution. However, in the presence of MEG molecules, an opposite result was observed in terms of the EC reading following MF exposure.

The reduction in EC may have been caused by exchanging the water cluster typically around mineral ions with MEG molecules. Therefore, the hydration shell could be replaced with bulky MEG molecules that alter the thickness of the solvation shell around ions (less water content), refer to Figure 6. As a result, the low hydration thickness and low solubility rate within 80 vol. % MEG solution lead to a greater scale formation tendency after exposure to MFs. The proposed hypothesis was based on the conclusions of Rozhkova, et al. [27] and Silva, et al. [16] as mentioned in the introductory section. As a result, the bulky ions generated a weaker EC measurement within 80 vol. % of MEG as shown in Figure 5. Moreover, exposure of the ionic species to the MF may not be the only factor influencing the hydration shell thickness due to the potential of MEG molecules to swap with the water molecules to form thicker solvation shell layers around ions.

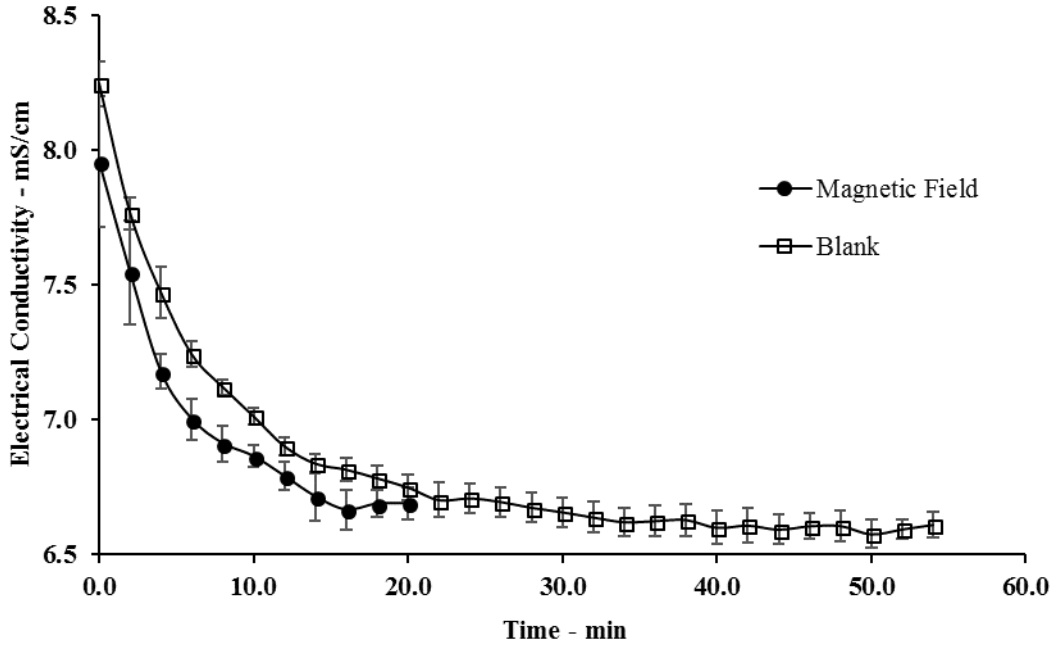


Figure 5 - Effect of MF exposure upon EC of equal concentration of $Ca^{2+}$ and $HCO_3^-$ solution within 80 vol. % MEG

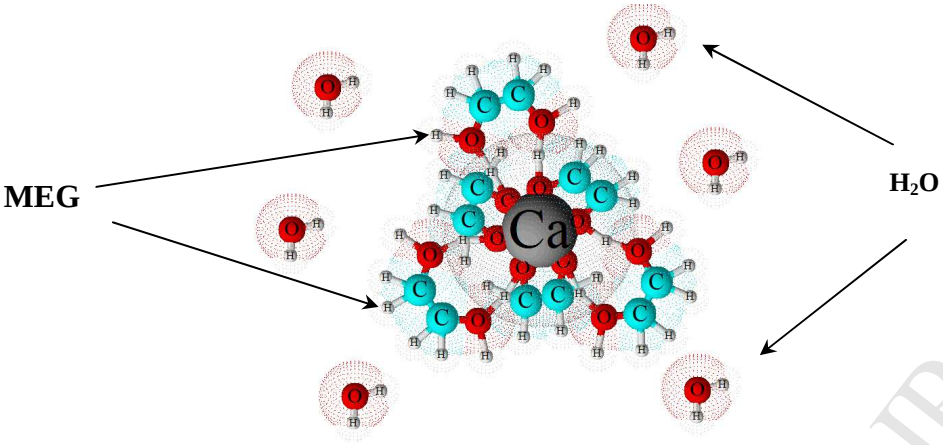


Figure 6 –Structure of the solvation shell with MEG molecules after exposure to MFs. The images were generated using ACD/ChemSketch Freeware software [33].

### 3.2 Influence of Magnetic fields on Scale Formation at 50 vol. % MEG Solution

Similarly to the performed 80 vol. % MEG trials, the performance of MF treatment on equal concentration $Ca^{2+}$ and $HCO_3^-$ 50 vol. % MEG solution has been conducted by monitoring ΔP across the capillary coil. A contrary result was observed for $CaCO_3$ formation in comparison to the trails performed using 80 vol. % MEG solutions as given in Figure 7. Within the 50 vol. % MEG solutions, the MF generated a positive effect after the fourth minute where the formation of the scale was inhibited in comparison to the blank trials leading to slower capillary tube blockage. The variation in scale formation behavior following MF exposure has highlighted an important difference in the performance of the MF treatment at varying MEG concentration. The adhesion of the deposits on the inner surface of the capillary coil was less frequent than the non-magnetized experiments. As such, it can be suggested that the inhibitory effect of MF treatment ultimately diminishes at higher MEG concentrations resulting in accelerated scale formation. The generated results are consistent with the findings of Higashitani and Oshitani [48] who reported opposite effects of the MF when increasing of methanol concentration.

Rozhkova, et al. [27] and Crupi, et al. [28] reported that the movement of MEG molecules within brine solution is higher than that in pure water. The increased movement of the MEG molecules was attributed to the rupture of a hydrogen bond typically formed between the water and MEG molecules. The presence of MEG solution leads to a significant reduction of the solubility index of ions resulting in a decrease of the saturation level and overall increasing scaling potential. However, when the rich MEG solution was exposed to the external MFs, the scale formation rate slowed, leading to a different scenario.

This scenario may have been caused by a decrease in solvation shell and an increase in the hydration shell thickness around the ionic species, therefore decreasing the potential for $CaCO_3$ scale formation [16]. Rozhkova, et al. [27] further concluded that the addition of mineral ions to the MEG + water system may weaken but not rupture the hydrogen bond between the OH-group of MEG molecules and the H-group of the water molecules. Therefore, exposure to the MFs within the 50 vol. % MEG trials are further contributing to the weakening of said OH-H bonds potentially leading to their rupture and reduction of the interaction of the MEG molecules and ionic species (refer to Figure 8). The potential weakening OH-H bonds between water and MEG resulted in a

significant increase in the measured EC readings following the MF exposure due to increase the ions solubility index.

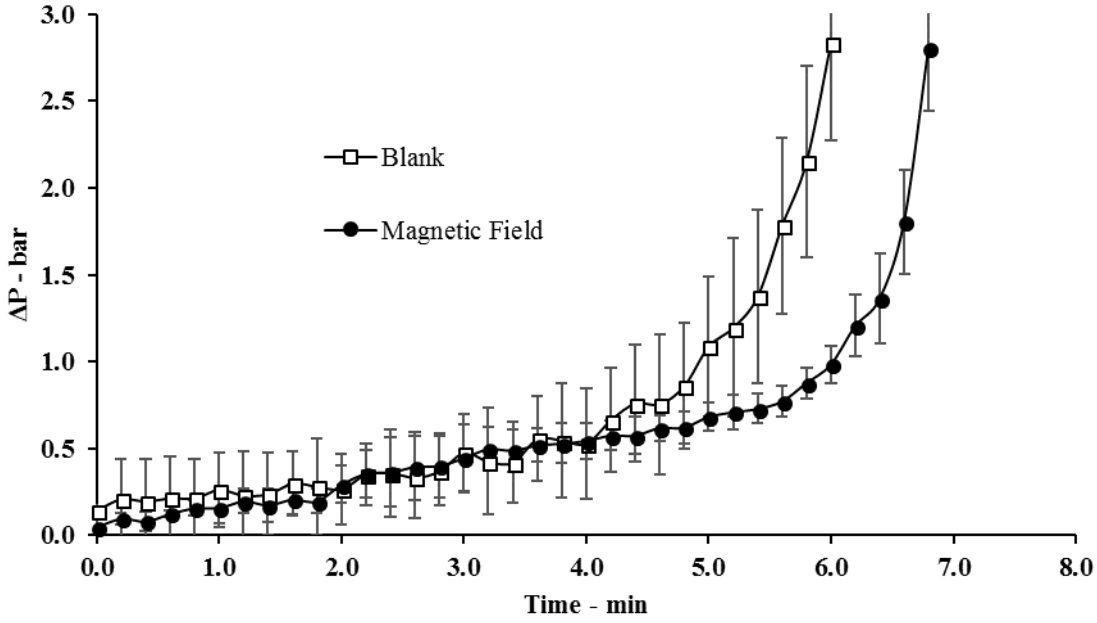


Figure 7 - Effect of MF exposure upon the tendency of equal concentration of $Ca^{2+}$ and $HCO_3^-$ solution within 50 vol. % MEG to form scale

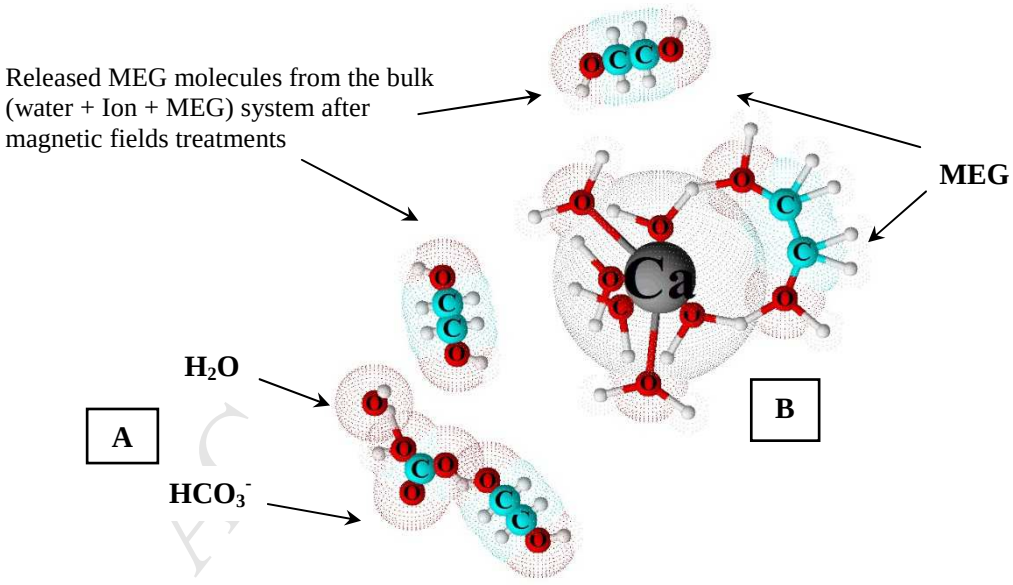


Figure 8 - (A) Structure of MEG – Bicarbonate ion - Water system at 50 vol. % MEG after MFs treatment, and (B) Structure of MEG – Calcium ion - Water system at 50 vol. % MEG after MFs treatment.

Figure 9 illustrates the differences in EC measurements of the exposed and blank trials within 50 vol. % MEG containing equal concentrations of $Ca^{2+}$ and $HCO_3^-$ ions. It is observed that exposure to the MF has initiated an increase in the measured EC when compared to the corresponding blank tests. In other words, it is apparent that applied external MFs exert an opposite effect on the number of water molecules and it's inter, and

intramolecular attraction compared to 80% by volume of MEG trials. Furthermore, the water–MEG molecules within the ions solvation shell followed a different arrangement pattern by keeping the water molecules inside the solvation shell leading to weakening the effect of bulky MEG molecules[43, 48].

In other words, these results indicate that the number of water molecules involved in the solvation shell was increased in a way that minimized the effect of MEG molecules. As a result, the external MF had a positive impact on rich MEG solution by attracting more water molecules into the solvation shell. The reason behind this behavior may be due to the smaller size of the water molecules compared to MEG molecules; this smaller size allows the water molecules to create more ion-dipole bonds with ions in the solution leading to a change in the hydration shell thickness and thus generating a different EC measurement. Since the EC measurement is dependent on the thermodynamic functions of hydration shell[41]. As shown in Figure 9, it can be observed that EC measurements after exposure to MFs confirm the decreasing in thickness of the solvation shell around the ionic species due to their inversely proportional relationship[31] and thus the increase in the hydration shell[16]. Furthermore, the effect of MFs within the 50 vol. % MEG has shown an inhibitory effect on the scale formation due to increasing the number of water molecules within its hydration shell.

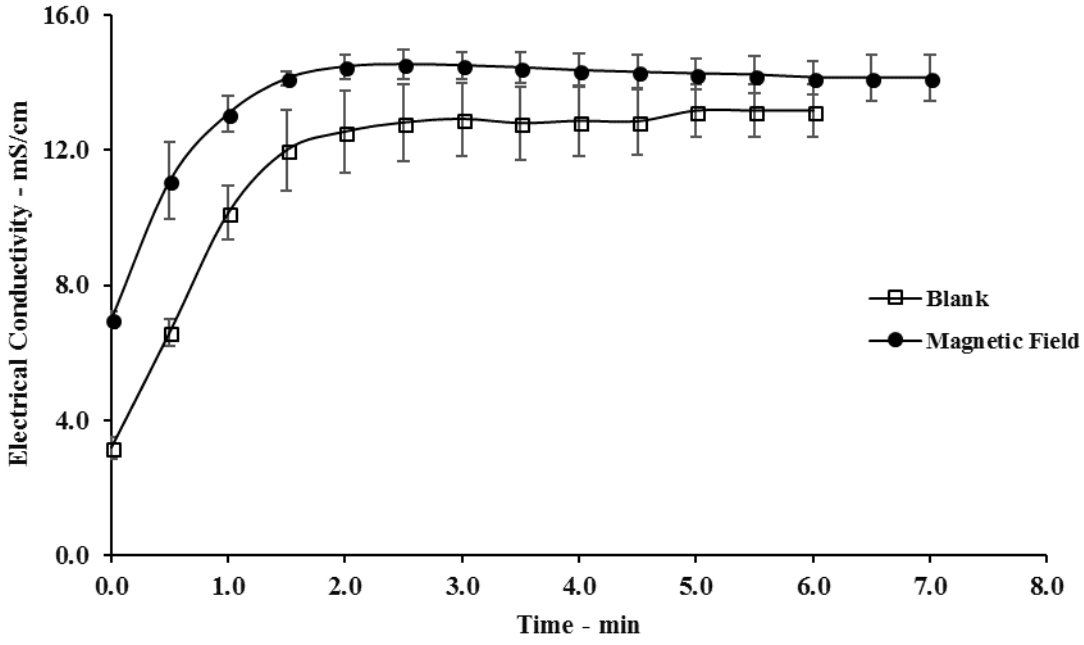


Figure 9 - Effect of MF exposure upon EC of equal concentration of $Ca^{2+}$ and $HCO_3^-$ solution within 50 vol. % MEG

### 3.3 Morphology of the Precipitates Calcium Carbonate after Exposed to External Magnetic Field

After evaluating the influence of MFs exposure on the scale formation behavior within 50 vol. % and 80 vol. % MEG solutions by using the DSL technique, as discussed in section 3.1. The morphology of the formed $CaCO_3$ has been investigated for both the exposed and blank trials. Furthermore, additional testing was performed by using the static jar technique to compare the produced $CaCO_3$ morphology with the results of DSL testing.

### 3.3.1 Crystal Structure of the Precipitates Calcium Carbonate at 50 and 80 vol. % MEG within DSL Technique

The SEM images of exposed and blank trials within 50 percent by volume MEG at 150°C are illustrated in Figure 10 A and B and Figure 11 where needle-like aragonite morphology was formed at both conditions. The trials with MFs present generated a noticeably longer needle structure at low magnification that appeared to be more singular in nature whereas the blank trials formed shorter needle structures that agglomerated to form a cluster of scale particles. The formation of aragonite at the testing conditions is consistent with the findings of Flaten, et al. [10] who stated that at 80°C and above, aragonite is the dominant morphology within all MEG concentrations.

Another interesting result has been observed as shown in Figure 11-A, where the precipitated $CaCO_3$ was slightly modified following MF treatment by forming dendritic cluster aragonite with a snowflake shape. Furthermore, the formation of the aragonite shape appeared to be nonstick and dry crystals. In contrast, the generated images for the blank tests highlight the formation of bulky aragonite spikes that are associated with other particles (refer to Figure 11-B). Additionally, it can be observed in the image (B) that a thick fluid combined with the generated crystals to form a non-regular surface or liquid-like post-nucleation clusters, as was also observed by Coey [49]. Moreover, image (B) shows the impact of the MF treatment on the size of $CaCO_3$ crystals whereby larger bulky crystals were formed when no MF treatment was applied during DSL trials.

It is also important to consider the effect of varying MEG concentration when evaluating the performance of MFs treatment to influence scale formation behavior. The scale-formation products generated within 80 vol. % MEG solution utilizing the DSL testing technique (refer to Figure 12) did not show any noticeable difference to that of corresponding 50 vol. % DSL testing following magnetic exposure (Figure 10 A and B). Furthermore, no impact on the scale morphology was observed after treatment with MFs in terms of shape, size, and structure within 80 vol. % MEG as shown in Figure 10 C and D and Figure 12, a result contrary to the corresponding 50 vol. % experiments where a small difference in the morphology was observed. This result suggests that the effect of the MF treatment in terms of the morphology formed is limited to solutions with equal or higher concentrations of water than MEG.

The reason behind this difference can be explained by the effect of the MF on the MEG-water molecules within the solvation shell of the dissolved ions. The effect of the applied MF alters the arrangement of the bulky MEG molecules within the hydration shell of the ion (refer to Figure 8) whereby the ion's hydration shell thickness is more likely to be influenced by the number of water molecules [27, 32]. The bonding energy between water molecules and the dissolved ions is greater than that between the ions and MEG molecules[27, 32]. This greater bonding energy between the water molecules and ions may hence facilitate their interaction leading to the formation of the scaling depicted by Figure 11 B. On the other hand, at higher MEG concentrations where the potential interaction of the ions and water molecules is limited, the drier singular dendritic clusters were formed regardless of if the MF was applied.

The scale formation layers generated with an irregular surface play an essential role in the accumulation of scale within fluid transportation pipelines. Therefore, using the MF treatment within 50 vol. % of MEG and heat exchangers' skin temperature may provide a method to prevent the formation of thick fluid substances and, hence scale, by creating a dry dendritic cluster aragonite structure of which is less likely to accumulate upon the

surface of thermal units and pipelines. As such, applying MF treatment to rich MEG solutions containing brine solutions could provide an economical and eco-friendly method to achieve scale formation control but not at 80% by volume of MEG.

**MF treatments trial, DSL** **Blank trial, DSL**

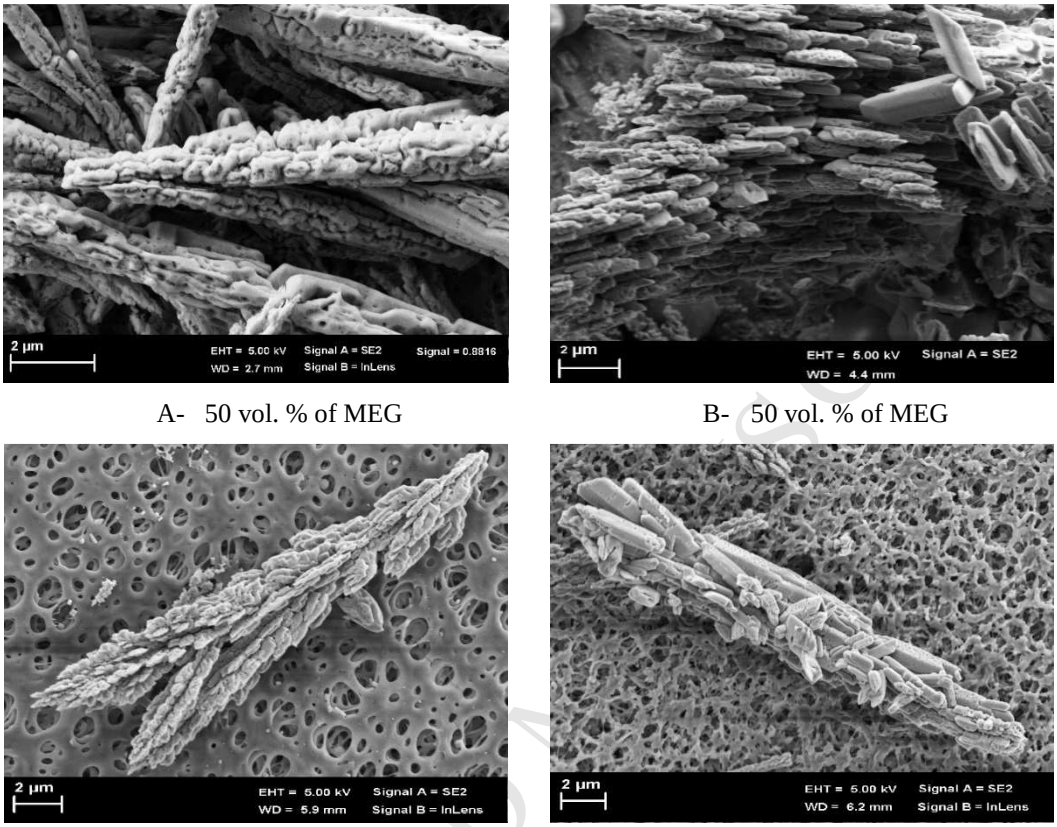


A- 50 vol. % of MEG B- 50 vol. % of MEG

C- 80 vol. % of MEG D- 80 vol. % of MEG

Figure 10 - SEM images of different MEG concentrations at 150℃ by using DSL technique.

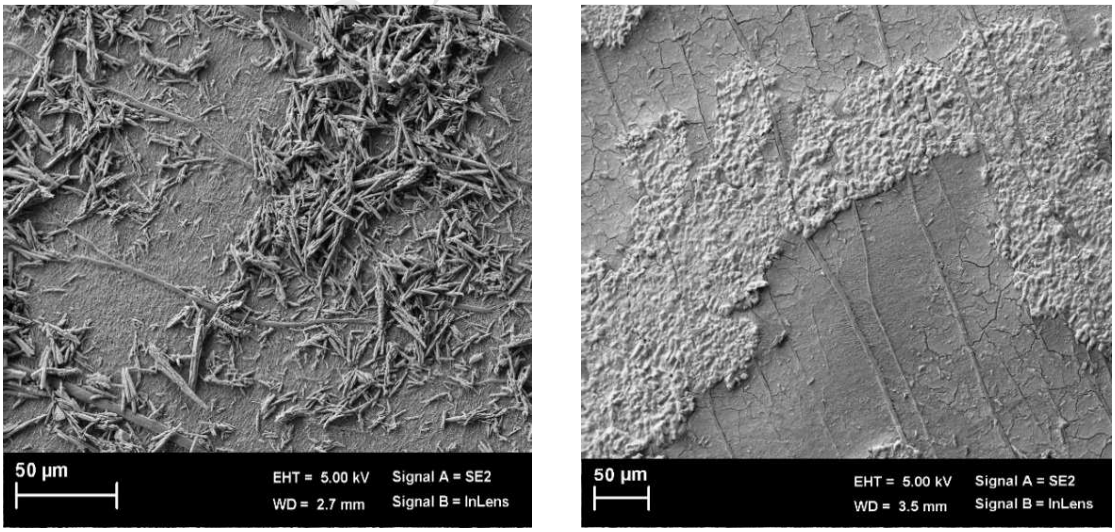


A- MF trial B- Blank trial

Figure 11 - Low magnification SEM images of 50 % by volume of MEG concentrations at 150°C by using DSL

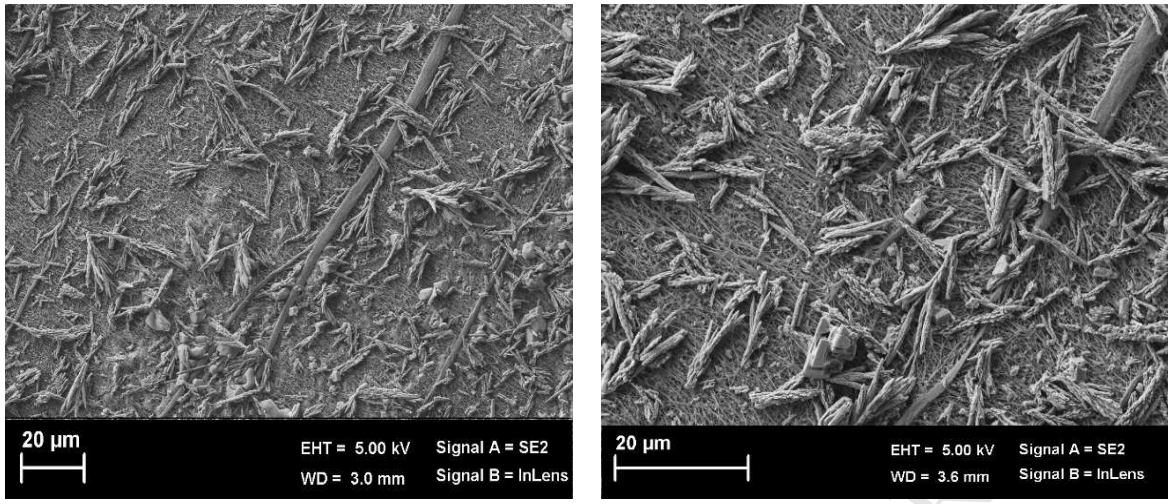


A- MF trial B- Blank trial

Figure 12 - High magnification SEM images of 80 % by volume of MEG concentrations at 150°C by using DSL

### 3.3.2 Crystal Structure of the Precipitates Calcium Carbonate at 50 and 80 vol. % MEG within Jar Cell Technique

Prior comparison of the jar test and DSL techniques for scaling evaluation have demonstrated that different $CaCO_3$ morphologies may be formed under the same conditions including temperature and composition[2, 50]. Furthermore, different nucleation rates and growth kinetics can also be expected during comparison of each analysis method[51]. It is well known that the nucleation rate and growth kinetics of $CaCO_3$ depends on both the system temperature and the supersaturation of the solutions [52]. According to kinetic studies of $CaCO_3$ formation, the nucleation process is more sensitive to the supersaturation level than the growth process[53-55]. Therefore, the nucleation process may form smaller $CaCO_3$ particles within high supersaturation conditions[51-52].

In such applications within aqueous solutions, Montazaud [56] have reported that the aragonite morphology is more likely to occur at a high temperature (>90°C). On the other hand, Cowan and Weintritt [57] concluded that aragonite could be observed at temperatures above 30°C. However, within MEG applications, Flaten, et al. [10] stated that the morphology of $CaCO_3$ may be influenced by increasing MEG content at 50°C with the conversion of aragonite to vaterite. The increase in MEG concentration may influence the supersaturation ratio of $CaCO_3$ at high temperatures hence influencing the nucleation process.

To compare the differences in morphology formed when applying the jar and DSL test methodologies, jar test experiments were conducted at 30°C and 150°C (±1°C) for varying MEG concentrations (0, 50 and 80 vol. %) using the same brine composition outlined by Table 2. The $CaCO_3$ scale at 0.0 percent by volume MEG within the jar test formed an abundance of idiomorphic calcite rhombohedra structure, which was the structure prevalent at room temperature (refer to Figure 13-A). Additionally, Figure 13-B shows SEM images of $CaCO_3$ morphology formed from aqueous solution within the jar tests at 150°C. The increase in temperature facilitated the formation of primarily idiomorphic calcite rhombohedral structures with non-smoothed surfaces. As a result, jar tests conducted as a part of this study were in line with the prior literature findings at 30 and 150°C[2, 24].

On the other hand, at 50 and 80% by volume of MEG, the morphologies of $CaCO_3$ produced during jar test experiments showed significantly different structures when compared to 0.0 vol. % of MEG trials, as shown in Figure 13C and E. The increase in MEG concentration had a significant impact on the type of crystal structure formed. It can be seen that vaterite crystals started to form at 30°C creating spherical shapes side by side with calcite within 50 vol.% of MEG as shown in Figure 13-C, while monoclinic and trigonal smooth surface shapes formed within 80 vol. % of MEG as shown in Figure 13-E. Upon raising the temperature to 150°C, a more complex assortment of crystals structures was found. Figure 13-D and F illustrate the formation of branched needle-like aragonite crystals in combination with idiomorphic calcite rhombohedra particles as identified by Flaten, et al. [10]. Moreover, Flaten, et al. [10] reported that vaterite particles should transition to aragonite crystals when the temperature was raised to approximately 80°C within 60% wt. of MEG solution a result consistent with the findings of this study. Therefore, the generated results can be explained by the action of the MEG solution itself, which changes the kinetic control of morphology structure with regards to the jar test technique.

Overall, the jar test results are in line with the results of Flaten, et al. [10] with regards to the needle-like $CaCO_3$ structure formed at approximately > 50 vol. % of MEG. However, of the tests conducted, significant differences in morphology of the scale formation are evidently illustrating the joint impact of both MEG concentration and temperature on scale formation growth. Further impact on the type and size of $CaCO_3$ scale formed is also apparently due to the dynamic nature of the DSL testing whereby the crystal structures are exposed to continuous liquid flow. In contrast to the static jar testing performed, non-branching needle-like aragonite crystals formed during DSL testing at 150°C exhibited a different geometric structure with a lack of calcite particles present. Due to the dynamic nature, the DSL testing methodology more closely simulates actual pipeline conditions whereby continuous liquid flow occurs. As such, the DSL method presents a more realistic approach to investigate scale formation within industrial applications and likewise the effect and evaluation of scale inhibitors.

**Trials at 30°C**

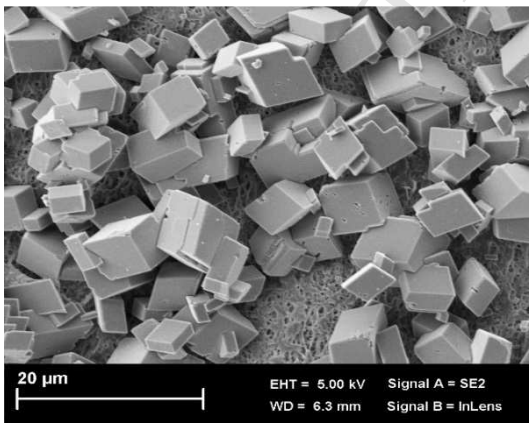


A- 0% by volume MEG, Jar cell technique

**Trials at 150°C**

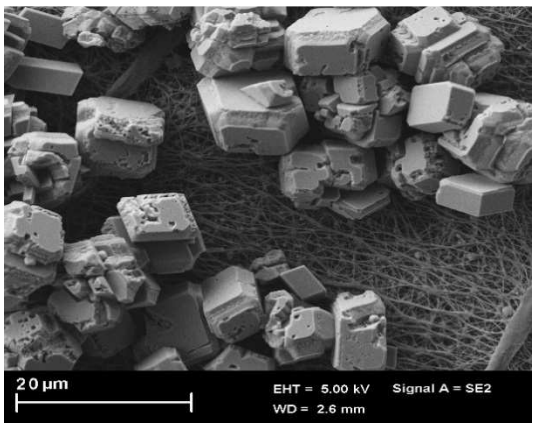


B- 0% by volume MEG, Jar cell technique

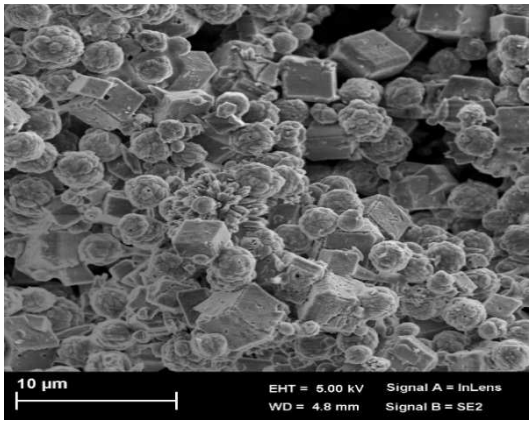


C- 50% by volume MEG, Jar cell technique

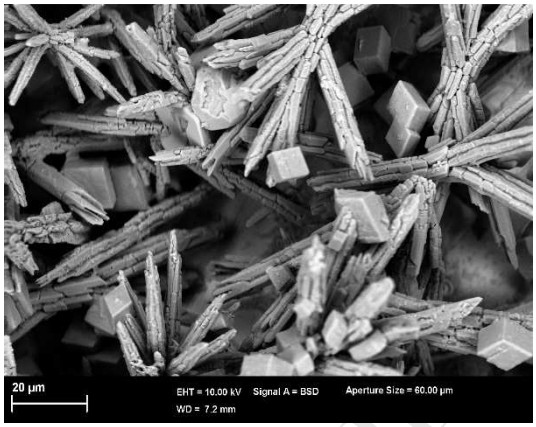


D- 50% by volume MEG, Jar cell technique

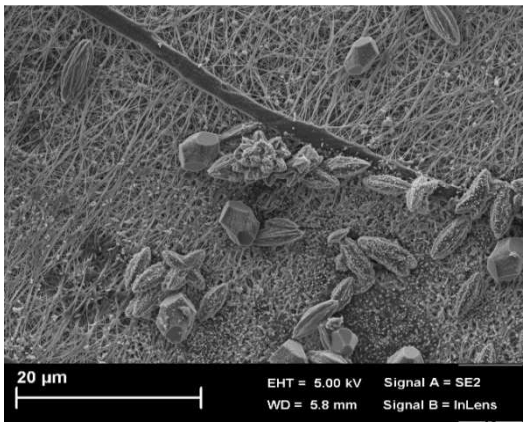


E- 80% by volume MEG, Jar cell technique

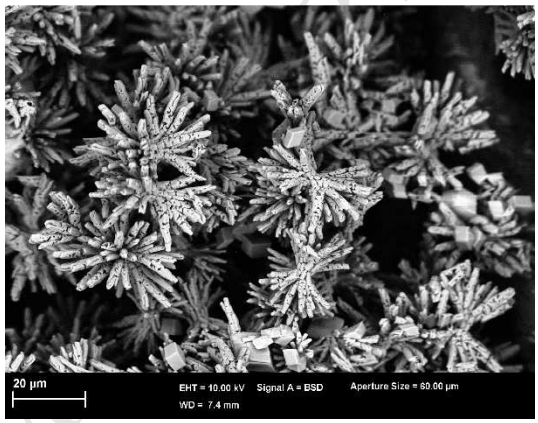


F- 80% by volume MEG, Jar cell technique

Figure 13 - SEM images of different MEG concentrations at 30 and 150°C by using Jar cell

### 3.4 Discussion of Mechanism caused after Exposure to Magnetic Fields

The influence of MFs on the strength of the intermolecular interactions in the aqueous system impacts on the hydration shell properties within the ionic solution[31, 44, 58-59]. Furthermore, the change in hydration shell thickness results in a change in EC due to an alteration in the number of $H_2O$ molecules in the first ion shell and ion mobility rate in watery system[1, 31, 41]. This hypothesis has been proven in several investigations within aqueous solutions, where the change in EC with hydration shell thickness was discussed[1, 31, 60].

Regarding the viscosity of MEG solutions, several studies have concluded that an increase in solution viscosity leads to lowered scale growth and nucleation rates[23-24, 61]. This is due to the significantly slower diffusion of growing particles within high viscosity solutions[24, 61]. Furthermore, according to the Nernst-Einstein equation, there is a relationship between fluid viscosity and its EC [62].

$$EC = \left(\frac{F^2}{R\,T}\right)\sum_i D_i z_i^2\,(\gamma_i)^a c_i \ldots 2$$

Where, F denotes Faraday's constant, T the temperature in Kelvin, R the gas constant and $z_i$ and $c_i$ the ionic species charge and molar concentration respectively. $D_i$ denotes to the self-diffusion coefficient of ions, which can be calculated by the Stokes-Einstein equation.

$$D_i = \frac{k_B\, T}{6\,\pi\,\mu\,r_i} \qquad \ldots 3$$

Where $k_B$ denotes Boltzmann's constant and $r_i$ is the solvation radius of ions. A clear correlation is thus evident between EC and the viscosity of solution due to its influence on the diffusion of ionic species through the solution (see Figure 14). As such, it can be expected that for higher MEG concentrations, a decrease in the measured EC would occur, consistent with Figure 14 for a range of 10 to 100 vol. % MEG concentration. However, further reduction in the EC occurred within the 80 vol. % MEG solutions following exposure to the MF in comparison to the blank tests (refer to Figure 5). The results can be further explained by the change in the radius of hydration and/or solvation shells around ions after exposure to the MFs as stated in the previous section.

According to equations 3, and 4, the solvation shell radius of ions is inversely proportional to the electrical conductivity, and self-diffusion coefficient. However, the activity coefficient of ions is proportional to the solvation shell ion radius. The best mathematical model to describe the relationship between the activity coefficient and solvation shell radius is the extended Debye-Hückel model[63], as shown in Equation 4.

$$log(\gamma_i) = -A * z_i^2 \left(\frac{\sqrt{I}}{1 + a_i * B\sqrt{I}}\right) \qquad \ldots 4$$

Where, *I*, is the ionic strength (mol/kg). The parameters A and B are constants and depend on the dielectric constant ($\varepsilon$) and temperature (T) as such: -

$$A = 1.82 * 10^6\,(\varepsilon * T)^{\frac{-3}{2}} \qquad \ldots 5$$

$$B = 50.3\,(\varepsilon * T)^{\frac{-1}{2}} \qquad \ldots 6$$

Therefore, the increase of the solvation shell radius (decreases the hydration shell) would result in the increase of ion pair formation would thus affect supersaturation with respect to calcium carbonate, as shown for the 80% MEG experiments. In contrast, the 50% MEG experiments showed a reduction in the scale formation rate due to a reduction of the solvation shell radius as indicated by the increased electrical conductivity, especially after exposure to the applied MF. Therefore, any change in the solvation shell radius influences the self-diffusion coefficient and the activity coefficient of ions and thus changes the scale formation rate. The influence of ions hydrated radius on the activity coefficient is illustrated in Figure 15.

Finally, it is essential to mention the dielectric constant that could be manipulated by external MFs thus impacting upon the Extended Debye-Hückel model (see the Equations 4 through 6). To be more precise in this hypothesis, Shen [64] reported that the dielectric constant of the electromagnetic field-treated water is 3.7% greater than the non-magnetized solutions, specifically under the extremely low electromagnetic field. While Pang and Shen [65] stated that the dielectric constant of the magnetized solution decreases with increasing the frequency of the applied electromagnetic field and exposure time. These proposed results indicate that the dialectic parameter can be affected by controlling the intensity of the MFs and the exposure time. The Extended Debye-Hückel model can estimate the ionic activity coefficient ($\gamma_i$) of ions by taking into consideration the radius of ions ($a_i$) and the dielectric constant of the solution[66-68]. However, the dielectric constant of water is higher than the

dielectric constant of MEG, by approximately a factor of two[22]. Therefore, the presence of external MFs could increase the dielectric constant of MEG-water solution, which in turn influences the ion activity and scaling potential. This phenomenon suggests the possible advantage of using MFs within scale formation treatments if it is used correctly.

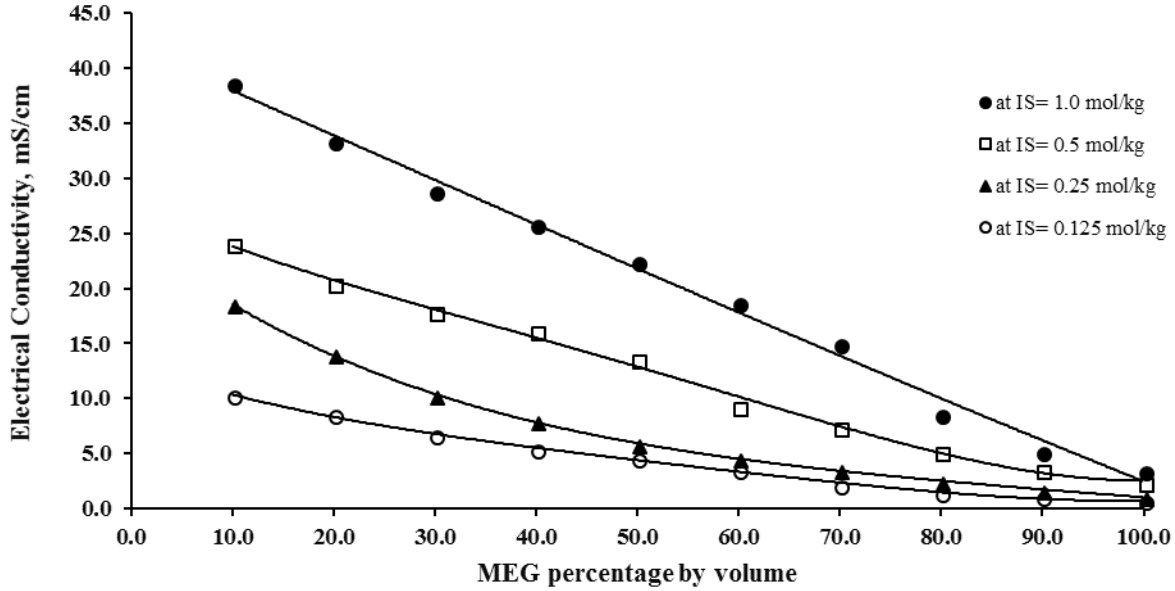


Figure 14 - EC of different MEG concentrations of varying ionic strength at 20°C

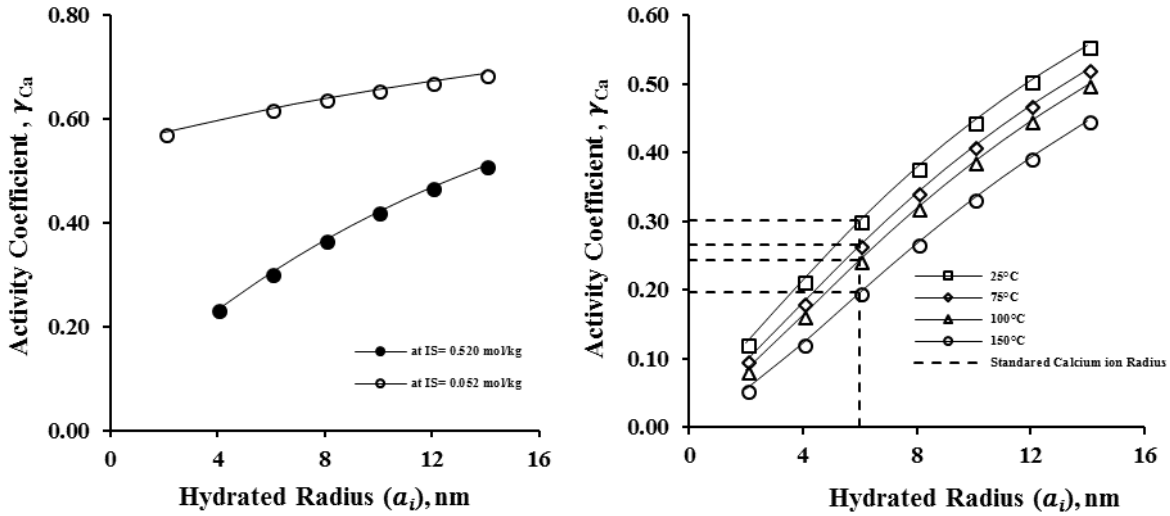


Figure 15 – Estimated activity coefficient of calcium ions as a function of ionic strength and temperature (using the extended Debye-Hückel model)

## 4.0 Conclusions

It was intended to use a high concentration of both calcium and carbonate ions in this study to make the deposition process inside the capillary faster so that we can observe the difference in magnetic field effects. Five

conclusions were reached concerning the applications of MF treatment in inhibiting the scale formation of $CaCO_3$ in aqueous solutions at different MEG concentrations. Firstly, the degree of scale formation, whether inhibited or promoted, is conditional on MEG content. Secondly, the exposure of the MEG + brine solutions to the applied MF had a significant impact on the EC measured. The results of the experiments conducted were consistent with previous studies of aqueous solutions where it was concluded that the solvation shell thickness of the $Ca^{2+}$ and $HCO_3^-$ ions were subject to manipulation by MFs leading to variations in EC [1, 31, 41]. Thirdly, following trials at 50 vol. % MEG concentration, bulky, and rough crystals were formed that may enhance a hypothesized clot-like build-up inside the transportation pipelines[1]. Similarly, jar tests highlighted the shift in crystallization processes that may occur at high MEG concentrations and high temperatures, although the jar test results cannot explain the morphology of real crystals in pipelines they can clarify the kinetic parameters that control crystals formed under different conditions.

Fourthly, previous studies suggested the external radius of ions to be the outer radius of hydration shells, not the actual ion radius in calculating the ionic activity coefficient[54, 66, 68]. This hypothesis has been reinforced after an improvement in the activity coefficient of ions occurring following exposure to MFs. Finally, due to the effective inhibition of scale formation produced by the external MF treatment within 50% by volume of MEG, it can be proposed that MF treatment could provide an environmentally friendly scale inhibition approach that could replace/reduce the use of traditional chemical inhibitors in industry. In this regard, we believe that research into the thermodynamic properties of an aqueous and non-aqueous solution in MFs is more promising.

## 5.0 Acknowledgment

The authors would like to acknowledge Curtin Corrosion Engineering Industry Centre (CCEIC) and the WA School of Mines: Minerals, Energy and Chemical Engineering at Curtin University for their support. Furthermore, I would like to thank Dr. Franca Jones for her important feedback which improved this work.

## 6.0 References

1. Al Helal, A.; Soames, A.; Gubner, R.; Iglauer, S.; Barifcani, A., Influence of Magnetic Fields on Calcium Carbonate Scaling in Aqueous Solutions at 150° C and 1 Bar. *Journal of Colloid and Interface Science* **2017**.

2. Amjad, Z., *The science and technology of industrial water treatment*. CRC Press: 2010.

3. Dickinson, S. R.; Henderson, G.; McGrath, K., Controlling the kinetic versus thermodynamic crystallisation of calcium carbonate. *Journal of Crystal Growth* **2002,** *244* (3), 369-378.

4. Moriarty, B. E.; Young, P. R.; Hoots, J. E.; Rasimas, J. In *Methods to monitor and control scale in cooling water systems*, CORROSION 2001, NACE International: 2001.

5. Babu, D.; Hosseinzadeh, M.; Ehsaninejad, A.; Babaei, R.; Kashkooli, M.; Akbary, H., Carbonates precipitation in MEG loops–A comparative study of South Pars and Bass Strait gas fields. *Journal of Natural Gas Science and Engineering* **2015,** *27*, 955-966.

6. Yong, A.; Obanijesu, E. O., Influence of natural gas production chemicals on scale production in MEG regeneration systems. *Chemical Engineering Science* **2015,** *130*, 172-182.

7. Yang, Q.; Liu, Y.; Gu, A.; Ding, J.; Shen, Z., Investigation of calcium carbonate scaling inhibition and scale morphology by AFM. *Journal of colloid and interface science* **2001,** *240* (2), 608-621.

8. Chilingar, G. V.; Mourhatch, R.; Al-Qahtani, G. D., *The Fundamentals of Corrosion and Scaling for Petroleum & Environmental Engineers*. Elsevier: 2013.

9. Muryanto, S.; Bayuseno, A.; Ma'mun, H.; Usamah, M., Calcium carbonate scale formation in pipes: effect of flow rates, temperature, and malic acid as additives on the mass and morphology of the scale. *Procedia Chemistry* **2014,** *9*, 69-76.

10. Flaten, E. M.; Seiersten, M.; Andreassen, J.-P., Polymorphism and morphology of calcium carbonate precipitated in mixed solvents of ethylene glycol and water. *Journal of Crystal Growth* **2009,** *311* (13), 3533-3538.

11. Gorna, K.; Hund, M.; Vučak, M.; Gröhn, F.; Wegner, G., Amorphous calcium carbonate in form of spherical nanosized particles and its application as fillers for polymers. *Materials Science and Engineering: A* **2008,** *477* (1), 217-225.

12. Dai, Z.; Kan, A. T.; Zhang, F.; Yan, F.; Ruan, G.; Bhandari, N.; Zhang, Z.; Liu, Y.; Al-Saiari, H. A.; Tomson, M. B. In *A Thermodynamic Model for The Solution Density and Mineral Solubility Predictions up to 250° C, 1,500 Bars for Na-K-Mg-Ca-Ba-Sr-Cl-CO 3-HCO 3-SO 4-CO 2 aq Systems*, SPE International Oilfield Scale Conference and Exhibition, Society of Petroleum Engineers: 2016.

13. Hu, Y.-B.; Wolthers, M. t.; Wolf-Gladrow, D. A.; Nehrke, G., Effect of pH and phosphate on calcium carbonate polymorphs precipitated at near-freezing temperature. *Crystal growth & design* **2015,** *15* (4), 1596-1601.

14. Baker, J. S.; Judd, S. J., Magnetic amelioration of scale formation. *Water Research* **1996,** *30* (2), 247-260.

15. Liu, X.; Chen, T.; Chen, P.; Montgomerie, H.; Hagen, T. H.; Wang, B.; Yang, X. In *Understanding Mechanisms of Scale inhibition Using Newly Developed Test Method and Developing Synergistic Combined Scale Inhibitors*, SPE International Conference on Oilfield Scale, Society of Petroleum Engineers: 2012.

16. Silva, I. B.; Neto, J. C. Q.; Petri, D. F., The effect of magnetic field on ion hydration and sulfate scale formation. *Colloids and Surfaces A: Physicochemical and Engineering Aspects* **2015,** *465*, 175-183.

17. Zaboon, S.; Soames, A.; Ghodkay, V.; Gubner, R.; Barifcani, A., Recovery of mono-ethylene glycol by distillation and the impact of dissolved salts evaluated through simulation of field data. *Journal of Natural Gas Science and Engineering* **2017,** *44*, 214-232.

18. Halvorsen, A. M. K.; Andersen, T. R.; Halvorsen, E. N.; Kojen, G. P.; Skar, J. I.; Biørnstad, C.; Fitje, H. In *The Relationship Between Internal Corrosion Control Method, Scale Control And Meg Handling Of A Multiphase Carbon Steel Pipeline Carrying Wet Gas With CO2 And Cetic Acid*, CORROSION 2007, NACE International: 2007.

19. AlHarooni, K.; Barifcani, A.; Pack, D.; Gubner, R.; Ghodkay, V., Inhibition effects of thermally degraded MEG on hydrate formation for gas systems. *Journal of Petroleum Science and Engineering* **2015,** *135*, 608-617.

20. Halvorsen, A. M. K.; Skar, J. I.; Reiersølmoen, K., Qualification of Scale And Corrosion Inhibitor For a Subsea HPHT Field With a MEG-loop. NACE International: 2012.

21. Halvorsen, A. M. K.; Andersen, T. R.; Halvorsen, E. N.; Kojen, G. P.; Skar, J. I.; Biørnstad, C.; Fitje, H., The Relationship Between Internal Corrosion Control Method, Scale Control And Meg Handling Of A Multiphase Carbon Steel Pipeline Carrying Wet Gas With CO2 And Cetic Acid. NACE International: 2007.

22. Sandengen, K. Prediction of mineral scale formation in wet gas condensate pipelines and in MEG (mono ethylene glycol) regeneration plants. Norwegian University of Science and Technology, 2006.

23. Hyllestad, K., Scaling of Calcium Carbonate on a Heated Surface in a Flow Through System with Mono Ethylene Glycol. **2013**.

24. Flaten, E. M.; Seiersten, M.; Andreassen, J.-P., Induction time studies of calcium carbonate in ethylene glycol and water. *Chemical Engineering Research and Design* **2010,** *88* (12), 1659-1668.

25. Flaten, E. M.; Ma, X.; Seiersten, M.; Aanonsen, C.; Beck, R.; Andreassen, J.-P. In *Impact of Monoethylene Glycol and Fe 2+ on Crystal Growth of CaCO 3*, CORROSION 2015, NACE International: 2015.

26. Tomson, M. B.; Fu, G.; Watson, M. A.; Kan, A. T., Mechanisms of Mineral Scale Inhibition. **2003**.

27. Rozhkova, M.; Rozhkova, A.; Butyrskaya, E., Separation of mineral salts and nonelectrolytes (ethylene glycol) by dialysis through ion-exchange membranes. *Journal of Analytical Chemistry* **2007,** *62* (8), 710-715.

28. Crupi, V.; Jannelli, M.; Maisano, G.; Majolino, D.; Migliardo, P.; Ponterio, R., Raman spectroscopic study of water in the poly (ethylene glycol) hydration shell. *Journal of molecular structure* **1996,** *381* (1), 207-212.

29. Matvejev, V.; Zizi, M.; Stiens, J., Hydration Shell Parameters of Aqueous Alcohols: THz Excess Absorption and Packing Density. *The Journal of Physical Chemistry B* **2012,** *116* (48), 14071-14077.

30. Tansel, B.; Sager, J.; Rector, T.; Garland, J.; Strayer, R. F.; Levine, L.; Roberts, M.; Hummerick, M.; Bauer, J., Significance of hydrated radius and hydration shells on ionic permeability during nanofiltration in dead end and cross flow modes. *Separation and Purification Technology* **2006,** *51* (1), 40-47.

31. Holysz, L.; Szczes, A.; Chibowski, E., Effects of a static magnetic field on water and electrolyte solutions. *Journal of Colloid and Interface Science* **2007,** *316* (2), 996-1002.

32. Rozhkova, A.; Butyrskaya, E.; Rozhkova, M.; Shaposhnik, V., Quantum chemical calculation of cation interaction with water molecules and ethylene glycol. *Journal of Structural Chemistry* **2007,** *48* (1), 166-169.

33. ACD/ChemSketch Freeware, A. C. D., Inc., Toronto, ON, Canada, www.acdlabs.com, 2015.

34. Bikkina, C.; Radhakrishnan, N.; Jaiswal, S.; Harrington, R.; Charlesworth, M. In *Development of MEG regeneration unit compatible corrosion inhibitor for wet gas systems*, SPE Asia Pacific Oil and Gas Conference and Exhibition, Society of Petroleum Engineers: 2012.

35. Ehsani, H. Influence of Monoethylene Glycol (MEG) on the corrosion inhibition of wet-gas flow lines. 2013.

36. Latta, T. M.; Seiersten, M. E.; Bufton, S. A. In *Flow assurance impacts on lean/rich MEG circuit chemistry and MEG regenerator/reclaimer design*, Offshore Technology Conference, Offshore Technology Conference: 2013.

37. Al Helal, A.; Soames, A.; Gubner, R.; Iglauer, S.; Barifcani, A., Measurement of mono ethylene glycol volume fraction at varying ionic strengths and temperatures. *Journal of Natural Gas Science and Engineering* **2018**.

38. Lide, D. R., CRC handbook of chemistry and physics. *12J204* **2004**.

39. Kochmarsky, V., Magnetic treatment of water: possible mechanisms and conditions for applications. *Physical Separation in Science and Engineering* **1996,** *7* (2), 77-107.

40. Madsen, H. L., Influence of magnetic field on the precipitation of some inorganic salts. *Journal of Crystal Growth* **1995,** *152* (1-2), 94-100.

41. Szczes, A.; Chibowski, E.; Hołysz, L.; Rafalski, P., Effects of static magnetic field on electrolyte solutions under kinetic condition. *The Journal of Physical Chemistry A* **2011,** *115* (21), 5449-5452.

42. Hasaani, A. S.; Hadi, Z. L.; Rasheed, K. A., Experimental Study of the Interaction of Magnetic Fields with Flowing Water. **2015**.

43. Chibowski, E.; Szcześ, A., Magnetic water treatment–a review of the latest approaches. *Chemosphere* **2018**.

44. Higashitani, K.; Kage, A.; Katamura, S.; Imai, K.; Hatade, S., Effects of a magnetic field on the formation of CaCO3 particles. *Journal of colloid and interface science* **1993,** *156* (1), 90-95.

45. Chang, K.-T.; Weng, C.-I., The effect of an external magnetic field on the structure of liquid water using molecular dynamics simulation. *Journal of Applied physics* **2006,** *100* (4), 043917.

46. Zhou, K.; Lu, G.; Zhou, Q.; Song, J.; Jiang, S.; Xia, H., Monte Carlo simulation of liquid water in a magnetic field. *Journal of Applied Physics* **2000,** *88* (4), 1802-1805.

47. Marcus, Y., Concentration dependence of ionic hydration numbers. *The Journal of Physical Chemistry B* **2014,** *118* (35), 10471-10476.

48. Higashitani, K.; Oshitani, J., Magnetic effects on thickness of adsorbed layer in aqueous solutions evaluated directly by atomic force microscope. *Journal of colloid and interface science* **1998,** *204* (2), 363-368.

49. Coey, J., Magnetic water treatment–how might it work? *Philosophical Magazine* **2012,** *92* (31), 3857-3865.

50. Boak, L. S. Factors that impact scale inhibitor mechanisms. Heriot-Watt University, 2013.

51. Jung, W. M.; Kang, S. H.; Kim, W.-S.; Choi, C. K., Particle morphology of calcium carbonate precipitated by gas–liquid reaction in a Couette–Taylor reactor. *Chemical engineering science* **2000,** *55* (4), 733-747.

52. Alamdari, A.; Saffari, M., Kinetic study of calcium carbonate precipitation in gas field brine containing methanol. *Journal of Natural Gas Science and Engineering* **2012,** *5*, 17-24.

53. Merkel, B.; Geochemistry, F. P. B. G., A practical Guide to modeling of Natural and Contaminated Aquatic Systems. *Volume* **2005,** *1*, 20.

54. Langmuir, D., *Aqueous environmental geochemistry*. 1997.

55. Plummer, L. N.; Busenberg, E., The solubilities of calcite, aragonite and vaterite in CO 2-H 2 O solutions between 0 and 90 C, and an evaluation of the aqueous model for the system CaCO 3-CO 2-H 2 O. *Geochimica et Cosmochimica Acta* **1982,** *46* (6), 1011-1040.

56. Montazaud, T., Precipitation of carbonates in the pretreatment process for regeneration of ethylene glycol. **2011**.

57. Cowan, J. C.; Weintritt, D. J., *Water-formed scale deposits*. Gulf Publishing Company, Book Division: 1976.

58. Schwierz, N.; Horinek, D.; Netz, R. R., Anionic and cationic Hofmeister effects on hydrophobic and hydrophilic surfaces. *Langmuir* **2013,** *29* (8), 2602-2614.

59. Collins, K. D., Ions from the Hofmeister series and osmolytes: effects on proteins in solution and in the crystallization process. *Methods* **2004,** *34* (3), 300-311.

60. Higashitani, K.; Iseri, H.; Okuhara, K.; Kage, A.; Hatade, S., Magnetic effects on zeta potential and diffusivity of nonmagnetic colloidal particles. *Journal of Colloid and Interface Science* **1995,** *172* (2), 383-388.

61. Flaten, E. M.; Seiersten, M.; Andreassen, J.-P., Growth of the calcium carbonate polymorph vaterite in mixtures of water and ethylene glycol at conditions of gas processing. *Journal of Crystal Growth* **2010,** *312* (7), 953-960.

62. Daintith, J., *A dictionary of chemistry*. OUP Oxford: 2008.

63. Hem, J. D. *Chemical equilibria and rates of manganese oxidation*; USGPO: 1963.

64. Shen, X. In *Increased dielectric constant in the water treated by extremely low frequency electromagnetic field and its possible biological implication*, Journal of Physics: Conference Series, IOP Publishing: 2011; p 012019.

65. Pang, X.-F.; Shen, G.-F., The changes of physical properties of water arising from the magnetic field and its mechanism. *Modern Physics Letters B* **2013,** *27* (31), 1350228.

66. Truesdell, A. H.; Jones, B. F., WATEQ, a computer program for calculating chemical equilibria of natural waters. *J. Res. US Geol. Surv* **1974,** *2* (2), 233-248.

67. Pitzer, K. S.; Simonson, J. M., Thermodynamics of multicomponent, miscible, ionic systems: theory and equations. *The Journal of Physical Chemistry* **1986,** *90* (13), 3005-3009.

68. Marcus, Y., Ionic radii in aqueous solutions. *Chemical Reviews* **1988,** *88* (8), 1475-1498.

- The study evaluates the magnetic fields (MF) performance in mono ethylene glycol (MEG)
- The dynamic scale loop was used to investigate the scale formation within MF
- The MEG regeneration conditions were used
- The MF performance was evaluated by monitoring pressure buildup and morphology
- The MF failed to inhibit scale formation at high MEG concentrations
- The MF succeeded in inhibiting the scale formation with 50 vol. % MEG